1

2

3 **TITLE**

4 Targeting T-cell receptor β-constant region for immunotherapy of T-cell malignancies

5

6

7 **AUTHORS**

8 Paul M. Maciocia[1], Patrycja A. Wawrzyniecka[1], Brian Philip[1], Ida Ricciardelli[2], Ayse

9 U. Akarca[1], Shimobi C. Onuoha[3], Mateusz Legut[4], David K. Cole[4], Andrew K.

10 Sewell[4], Giuseppe Gritti[5], Joan Somja[6], Miguel A. Piris[7], Karl S. Peggs[1], David C.

11 Linch[1], Teresa Marafioti[1], Martin A. Pule[1,3]*

12

13 [1] University College London, Cancer Institute, London, UK

14 [2] University College London, Institute of Child Health, London, UK

15 [3] Autolus Ltd, London, UK

16 [4] Division of Infection and Immunity, Cardiff University School of Medicine, Cardiff,

17 UK

18 [5] Hematology and Bone Marrow Transplant Units, Papa Giovanni XXIII Hospital,

19 Bergamo, Italy

20 [6] Department of Anatomy and Cellular Pathology, University of Liege, Belgium

21 [7] Department of Pathology, Fundacion Jimenez Diaz, CIBERONC, Madrid, Spain

22

23

24 * Corresponding author

25

26

27 **ABSTRACT**

28

29 Mature T-cell cancers are typically aggressive, treatment-resistant and associated

30 with poor prognosis. Translation of immunotherapeutic approaches has been limited

31 by a lack of target antigens discriminating malignant from healthy T-cells. Unlike B-

32 cell depletion, pan T-cell aplasia is prohibitively toxic. We report a novel targeting

33 strategy based on the mutually exclusive expression of either *TRBC1* or *TRBC2* T-

34 cell receptor (TCR) β-constant domain. We identify an antibody with unique TRBC1

35 specificity, and use this to demonstrate that while normal and viral-specific T-cells

36 contain TRBC1 and TRBC2 compartments, malignancies are restricted to only one.

37 As proof of concept for anti-TRBC immunotherapy, we developed anti-TRBC1

38 CART-cells, which recognise and kill normal and malignant TRBC1 but not TRBC2

39 T-cells, *in vitro* and in a disseminated murine leukaemia model. Unlike non-selective

40 approaches targeting the entire T-cell population, TRBC-targeted immunotherapy

41 could eradicate a T-cell malignancy while preserving sufficient normal T-cells to

42 maintain cellular immunity.

43

44

45

46

47 **INTRODUCTION**

48

49 Mature T-cell lymphomas (PTCLs) are a heterogeneous group of disorders,

50 collectively comprising 10-15% of non-Hodgkin's lymphoma[1]. These cancers typically

51 behave aggressively[2,3]. Outcomes are worse than equivalent B-cell cancers, with an

52 overall estimated 5-year survival of only 32%[3]. Furthermore, while treatment of B-cell

53 cancers benefits from targeted immunotherapies such as therapeutic monoclonal

54 antibodies (mAbs)[4], bispecific T-cell engagers[5] and more recently chimeric antigen

55 receptor (CAR) T-cell therapy[6,7], no such approaches are available for T-cell cancers.

56

57 Immunotherapies used in B-cell malignancies target pan B-cell antigens, since no

58 antigens exist which discriminate normal from malignant B-cells. The consequent

59 depletion of the normal B-cell compartment is surprisingly well tolerated and is

60 considered an acceptable side-effect[6,7]. The situation is different with T-cells: once

61 again, no antigens exist which discriminate normal from malignant T-cells[3,8];

62 however, T-cell aplasia consequent to targeting a pan T-cell antigen would lead to

63 profound and unacceptable immunosuppression[9]. Here, we describe a targeting

64 approach for treating mature T-cell cancers which relies on recognition of a pan T-

65 cell antigen, but avoid severe immunosuppression.

66

67 The α/β T-cell receptor (TCR) is a pan T-cell antigen. Apart from its expression on

68 normal T-cells it is a highly promising target for PTCL: it is expressed by >95% of

69 cases of PTCL-NOS[8], almost all AITL[8], as well as 30% of T-acute lymphoblastic

70 leukaemia (T-ALL)[10]. High and homogenous surface expression is commonly seen

71 on lymphoma cells[11] and in addition, evidence exists that a proportion of PTCL cases

72 may depend on TCR-associated signalling for lymphomagenesis and survival[12].

73

74 TCR α and β chains comprise amino-terminal variable and carboxy-terminal constant

75 regions[13] (Figure 1a). TCR diversity is generated by somatic recombination, when

76 each TCR chain selects a variable (V), diversity (D), joining (J) and constant (C)

77 region[13]. Importantly, cells of a clonal T-cell population all express the same unique

78 TCR. However, approaches targeting TCR variable regions unique to a malignant

79 clone are impracticable, since a bespoke therapeutic is required for each patient.

80

81 An oft-forgotten feature of TCR β-chain recombination is that there are two β-

82 constant region genes: TRBC1 and TRBC2. Each TCR (and therefore each T-cell)

83 expresses, mutually exclusively and irreversibly, TCR β-constant region coded by

84   either TRBC1 or TRBC2[14,15] (Figure 1b). Hence, normal T-cells will be a mixture of

85   individual cells expressing either TRBC1 or 2, while a T-cell cancer will express

86   either TRBC1 or 2 in its entirety. We propose targeting TRBC1 in case of a TRBC1+

87   T-cell malignancy, or the converse in case of a TRBC2+ malignancy. This will target

88   all cells of the malignant clone, but leave a substantial proportion of the T-cell

89   compartment intact.

90

91   In this work, we demonstrate that it is possible to distinguish between TRBC1 and 2

92   TCRs with an antibody, despite almost identical amino acid sequences (Figure 1c).

93   We show that peripheral blood T-cells in normal subjects comprise of a mixture of

94   approximately 35:65% TRBC1:2 cells, and that complete depletion of either TRBC1

95   or 2 compartments will still maintain considerable anti-viral repertoire. We confirm

96   TRBC monoclonality in many types of T-cell malignancies by both flow cytometry and

97   immunohistochemistry. Finally, we demonstrate efficacy of a CAR with TRBC1

98   specificity to prove our targeting concept.

99

100

101   **RESULTS**

102

103   **JOVI-1 mAb is specific for TRBC1-expressing cells**

104

105   To find a TRBC-specific binder, we screened anti-TCR mAbs which are known to

106   bind a proportion of T-cells in peripheral blood. In order to screen for TRBC1/2

107   specificity we cloned the α and β-chains of the well-characterised HA-1 TCR[16] in

108   TRBC2 (native) format or with mutations introduced in the constant domain to

109   convert to TRBC1. We stably expressed either TCR on the surface of Jurkat T-cell

110   line with knocked out TCR α and β loci (JKO). Analysis by flow cytometry

111   demonstrated that, while both TRBC1-JKO and TRBC2-JKO lines expressed surface

112   TCR/CD3, mAb JOVI-1[17] recognised only TRBC1-JKO cells and not TRBC2-JKO

113   cells (Figure 1d), confirming the TRBC1 specificity of this antibody. Surface plasmon

114   resonance analysis demonstrated that JOVI-1 bound to a TRBC1-TCR with an

115   affinity of K_D = 0.42nM and a half-life of ~30mins, in line with other therapeutic

116   antibodies[18]. In contrast, JOVI-1 binding to a TRBC2-TCR was >10,000x weaker,

117   demonstrating the remarkable specificity of the reagent (supplementary Figure 1).

118

119   TCR β-junctional regions segregate with constant domains: TCRs selecting TRBJ1

120   1-6 use TRBC1, and those selecting TRBJ2 1-7 use TRBC2[13]. It was therefore

121   possible that JOVI-1 only maintains TRBC1-specificity in the context of particular

122   junctional regions. We cloned several TCRs of varying antigen specificity, utilising a

123   range of variable/ junctional regions, from publicly available sequences. When

124   transfected into human embryonic kidney (HEK)-293T cells along with a plasmid

125   supplying the components of CD3, TCRs were expressed on the cell surface. JOVI-1

126   uniformly recognised TRBC1 cells despite varying TRBJ1 regions, and did not

127   recognise cells expressing TRBC2 TCRs and varying TRBJ2 regions (Figure 1e). In

128   addition, we cloned a truncated TCR lacking α and β V(D)J domains and stably

129   expressed this on the surface of JKO cells. CD3 staining confirmed surface

130   assembly, and staining with JOVI-1 was similar to that seen with full-length TCR

131   (Figure 1f). This offered further confirmation that junctional regions were not required

132   for the JOVI-1 epitope.

133

134   We then sought to determine the residues of TRBC responsible for the TRBC1-

135   specificity of JOVI-1. Structural analysis suggested that the F->Y at residue 36 is

136   buried in secondary structure and V->E at residue 135 is likely too close to the

137   membrane to be accessible. However, the NK->KN difference at residues 4-5 is

138 exposed to the surface and represents a substantial difference of both shape and

139 charge to the epitope. By introducing each mutation required to convert TRBC2 to

140 TRBC1 individually, then stably expressing these constructs on the surface of JKO

141 cells, we confirmed that the reversal of asparagine and lysine residues at positions 4-

142 5 was indeed the discriminating portion of the JOVI-1 epitope (Figure 1f,g).

143

144

145 **Normal αβ T-cells contain a mixture of TRBC1+ and TRBC1- populations**

146

147 Using JOVI-1, we then sought to determine the proportion of T-cells from normal

148 donors that were TRBC1 versus TRBC2. Each donor had TCR+TRBC1-positive and

149 TCR+TRBC1-negative cells in both CD4 and CD8 compartments, with median

150 TRBC1 expression of 35% (range 25-47%, Figure 2a,b). We also confirmed that CD4

151 and CD8 differentiation subsets all contained both populations with a similar

152 TRBC1:TRBC2 ratio (Suppl Fig 2a,d). In addition, we identified 2 cell types which

153 express a semi-invariant restricted TCR repertoire, mucosal-associated invariant T-

154 cells (MAITs, suppl Fig 2b,d) and invariant natural killer/ T-cells (iNKTs, suppl Fig

155 2c,d) and demonstrated that these populations also contain both TRBC1-positive

156 and TRBC1-negative cells, albeit with a lower TRBC1 proportion than seen in bulk T-

157 cell populations.

158

159 Although the polyclonal T-cell population in normal donors contained both TRBC1

160 and TRBC2 cells, we reasoned that the T-cell response to a particular virus may be

161 skewed towards one of these, and therefore that removal of one subset could result

162 in loss of cellular immunity. To determine if this was the case, we generated

163 oligoclonal Epstein Barr Virus (EBV)-specific cytotoxic T-cell lines from normal

164 donors, as previously described[19] (Supplementary Figure 3a). These cells lysed

165 autologous EBV-transformed cells (Supplementary Figure 3b). Staining in 3 donors

166 revealed the cells were >98% CD8+ (data not shown) and contained a mixed

167 population of TRBC1-positive and TRBC1-negative (median 45% TRBC1-positive)

168 cells (Supplementary Figure 3c), demonstrating that the T-cell response to EBV

169 contains both populations (Figure 2c). In addition, we identified T-cells specific for

170 cytomegalovirus (CMV) or adenovirus (AdV) by incubation of peripheral blood

171 mononuclear cells (PBMCs) with pools of antigenic peptides. Viral-specific T-cells,

172 identified by interferon-gamma (IFN-γ) expression after peptide incubation

173 (Supplementary Figure 3d), were found to contain both TRBC1-positive and TRBC1-

174 negative cells (Figure 2d). Summary data from normal donors demonstrated median

175 TRBC1 expression of 45% (CMV) and 41% (AdV) (Figure 2e).

176

177

178 **T-cell derived malignant cell lines and primary T-cell tumours are clonally**

179 **TRBC1+ or TRBC1-**

180

181 Surface TCR+ cell lines were stained with JOVI-1 and were found to be either

182 TRBC1-positive (H9, Jurkat, MJ) or TRBC1-negative (HD-Mar2, HPB-ALL, T-ALL1,

183 HH, T-ALL1). TRBC1 versus TRBC2 expression was confirmed at the transcriptional

184 level by PCR amplification of the β-constant region from cDNA, followed by Sanger

185 sequencing (Figure 3a). These data confirmed JOVI-1 as a marker of TRBC1

186 monoclonality in cell lines. Next, using multiparameter flow cytometry, we analysed

187 primary blood samples from several patients with T-large granular leukaemia (T-

188 LGL), a TCR+ lymphoproliferative disorder characterised by circulating tumour cells

189 which express CD57[20]. While CD57+ tumour cells demonstrated markedly skewed

190 TRBC1:TRBC2 ratios, normal CD4 and CD8 T-cells displayed appropriate ratios of

191 each population (Figure 3b). Using intracellular staining, we replicated this finding in

192 primary marrow samples of T-ALL (Figure 3c). Further, using flow cytometry (FACS)

193 or immunohistochemistry (IHC) on frozen tissue sections, we stained a number of

194 primary samples of TCR+ malignancies of multiple histologies and confirmed that

195 TRBC1 staining could be used to determine if cancer cells were clonally TRBC1-

196 positive or TRBC1-negative (Figure 3d,e). In 57 samples (38 analysed by IHC, 19 by

197 FACS), 39% were TRBC1-positive and 61% were TRBC1-negative (Table 1). Of

198 note, TCR/CD3 expression assayed by FACS in primary malignancies was typically

199 at a similar level to normal T-cells from the same patient (median MFI = 96% of

200 normal T-cell MFI), other than in adult T-cell leukaemia/ lymphoma (ATLL) where

201 expression was typically dimmer than in normal T-cells (median MFI 23% of normal

202 T-cell MFI, Fig 3f).

203

204 **T-cells transduced with anti-TRBC1 CAR specifically target TRBC1+ but not**

205 **TRBC2+ cells** *in vitro*

206

207 As a proof of concept for therapies targeting TRBC we cloned a single-chain variable

208 fragment based on the JOVI-1 antibody into a 3rd generation CAR format[21]. We

209 retrovirally transduced T-cells from normal donors to stably express this construct,

210 and confirmed surface expression of CAR on up to 90% of cells (Fig 4a). We

211   subsequently co-cultured non-transduced (NT) or anti-TRBC1 CAR T-cells with NT-

212   JKO, TRBC1-JKO or TRBC2-JKO cells. While NT effectors did not secrete IFN-γ in

213   response to any target cells, TRBC1 CAR T-cells specifically secreted IFN-γ only

214   when incubated with TRBC1-JKO and not NT-JKO or TRBC2-JKO cells (Figure

215   4b,c). In 4hr chromium release cytotoxicity assays, NT cells did not display

216   cytotoxicity, while anti-TRBC1 CAR T-cells specifically killed TRBC1-JKO and not

217   NT-JKO or TRBC2-JKO cells (Figure 4d,e).

218

219   In addition, we performed flow cytometric cytotoxicity assays using multiple α/ β

220   TCR+ cell lines as targets, and confirmed killing of cells expressing TRBC1-TCRs but

221   not TRBC2-TCRs by anti-TRBC1 CAR T-cells, while NT T-cells did not lyse either

222   (Figure 4f). Next, to simulate a physiological setting, we mixed TRBC1-JKO cells

223   labelled with CD19 marker gene at 1:1 ratio with TRBC2-JKO cells labelled with blue

224   fluorescent protein (BFP). This population was co-cultured with anti-TRBC1 CAR-T

225   or NT cells. Analysis at 48hrs confirmed eradication of TRBC1 cells with preservation

226   of TRBC2 cells by anti-TRBC1 CAR, and no killing of either population seen with NT

227   effectors (Figure 4g).

228

229   We obtained primary malignant cells from multiple patients with TRBC1-positive T-

230   cell malignancies. We co-cultured patient neoplastic cells with NT or anti-TRBC1

231   CART-cells at a 1:1 ratio. Using allogeneic T-cells, we demonstrated specific kill of

232   malignant cells in cases of T-prolymphocytic leukaemia (T-PLL) and PTCL-NOS, with

233   preservation of a substantial proportion of residual normal T-cells (Figure 4h).

234   Malignant cell killing was seen even in cases of ATLL (Figure 4i,l), where TCR/CD3

235   was partially downregulated from the cell surface (Figure 3f). In addition, we

236   demonstrated successful transduction of T-cells from a patient with TRBC1+

237   malignancy (ATLL) despite heavy circulating ATLL burden (Figure 4j), that the T-cell

238   product was 'purged' of contaminating ATLL cells (Figure 4k) and that anti-TRBC1

239   CAR specifically killed autologous ATLL cells (Figure 4l).

240

241   **Anti-TRBC1 CAR-T cells selectively deplete normal TRBC1, but not TRBC2**

242   **cells**

243

244   Following anti-TRBC1 CAR transduction, no TRBC1+ cells could be detected in

245   either the transduced or non-transduced fractions, indicating possible depletion of

246   this population (Supplementary Fig 4a). However, we reasoned that absent TRBC1

8

247 staining was likely due to epitope blocking by ligated anti-TRBC1 CAR. Therefore,

248 we transduced cells with anti-TRBC1 CAR and CD34 marker gene[22]. This enabled

249 sorting of cells into CAR-positive and CAR-negative fractions using CD34-bead

250 magnetic depletion. We confirmed depletion of all CAR+ cells in the negative fraction,

251 thus excluding any effect of epitope blockade by CAR. While NT cells contained

252 both TRBC1-positive and TRBC1-negative fractions, the CAR-negative fraction did

253 not contain any TRBC1-positive cells, confirming selective depletion of TRBC1 cells

254 (Supplementary Figure 4b). Further, we sorted normal donor T-cells into TRBC1-

255 positive and TRBC1- negative populations using magnetic beads. We subsequently

256 separately labelled each population with different fluorescent nuclear dyes, enabling

257 later discrimination of the populations, and co-cultured with autologous NT or anti-

258 TRBC1 CART-cells. While TRBC2 cells co-cultured with anti-TRBC1 CAR were not

259 depleted compared to NT condition, TRBC1 cells were 80% depleted at 7 days

260 (Supplementary Figure 4c), indicating selective purging of this population. This was

261 confirmed in a further assay, in which TRBC1 cells were mixed at a 1:2

262 (physiological) ratio with TRBC2 cells before 1:1 co-culture with NT or anti-TRBC1

263 cells. At 7 days, virtually all TRBC1 cells had been depleted from the culture, while

264 TRBC2 cells remained (Supplementary Fig 4d). Finally, to further mitigate against

265 potential transduction of contaminating TRBC1 tumour cells, we pre-depleted normal

266 donor T-cells of TRBC1-positive cells to obtain cells which were >99% TRBC1-

267 negative (Supplementary Figure 4e), then demonstrated transduction with anti-

268 TRBC1 CAR that was similar to that achieved for unsorted cells (Supplementary

269 Figure 4f).

270

271

272 **Anti-TRBC1 CAR-T cells are specific and effective in murine models of**

273 **disseminated T-cell malignancy.**

274

275 Non-obese diabetic-severe combined immunodeficiency γ-chain–deficient (NSG)

276 mice (Jackson) were intravenously injected with Jurkat T-cells, which natively

277 express a TRBC1 TCR at a level similar to primary tumour and normal T-cells

278 (Figure 2g). Jurkat cells were modified to stably express firefly luciferase (F-Luc) and

279 CD19 marker gene, and stably engrafted in the bone marrow of all injected animals

280 by day 6 (Figure 5a,b). Following engraftment, we treated mice with T-cells

281 expressing anti-TRBC1 CAR or a control (irrelevant) CAR. Mice treated with anti-

282 TRBC1 CAR had dramatic reduction of Jurkat cell burden by BLI at D10 (Figure

283 5b,c), and this was associated with a substantial survival benefit. In a further

284   experiment to evaluate CAR persistence (Figure 5e), we demonstrated Jurkat cell
285   clearance and increased numbers of anti-TRBC1 versus control CAR T-cells in
286   peripheral blood at D21 following T-cell injection (Figure 5f). Bone marrow was
287   harvested at the time of death (survivors culled at D42), with similar results seen
288   (Figure 5g).

289

290   Next, we injected a further cohort of mice with equal proportions of Jurkat-TRBC1
291   cells (human CD19 marker gene) and JKO cells engineered to express TRBC2 TCR
292   and BFP marker gene). Jurkat cell engraftment in marrow was confirmed in all
293   animals by BLI at day 6. Animals were then treated with NT or anti-TRBC1 CAR T-
294   cells. Flow cytometry of bone marrow confirmed the TRBC1 specificity of anti-TRBC1
295   CAR T-cells *in vivo*: while mice receiving NT effectors had approximately equal
296   proportions of Jurkat-TRBC1 and JKO-TRBC2 cells in marrow, only JKO-TRBC2
297   cells were seen in recipients of anti-TRBC1 CAR T-cells (Figure 5e,f).

298

299   Finally, in order to determine if anti-TRBC1 CAR was able to deplete TRBC1-Jurkat
300   in a physiological setting (ie in the presence of normal T-cells), we engrafted NSG
301   mice with Jurkat-CD19-Fluc cells as before. After 7 days, mice were injected with
302   human PBMCs (Supplementary Figure 5a). After a further 7 days, human monocyte
303   and T-cell engraftment was confirmed by flow cytometry of peripheral blood
304   (Supplementary Figure 5b), and progressive disease was demonstrated by BLI
305   (Supplementary Figure 5c). Animals were then injected with anti-TRBC1 CAR or
306   control CAR, with cells prepared from the same donor as initial PBMCs. BLI and flow
307   cytometry of bone marrow at 5 days following treatment demonstrated Jurkat cell
308   control in anti-TRBC1 CAR recipients, but progression in control CAR recipients
309   (Supplementary Figure 5c,d,e). Flow cytometry of bone marrow (Supplementary
310   Figure 5e) and spleen (Supplementary Figure 5f) at D6 demonstrated similar
311   numbers of non-CAR T-cells were present in anti-TRBC1 and control CAR recipients,
312   confirming persistence of normal T-cells in the face of Jurkat cell depletion.

313
314
315
316

317 **DISCUSSION**

318

319 The presence of two functionally identical genes at the TCR-β constant region has

320 been recognised for more than 30 years[14,15], but has not been exploited until now.

321 We have demonstrated that despite highly similar amino acid sequences, it is

322 possible to discriminate between TRBC1 and TRBC2 proteins on normal and

323 malignant T-cells. Indeed, JOVI-1 demonstrated >10,000-fold difference in binding

324 affinity, with specificity based on the reversal of only 2 residues in TRBC. Consistent

325 with previous findings, we have shown that approximately 2/3 of both normal T-

326 cells[23,24] and T-cell cancers[25] express TRBC2-TCR.

327

328 We believe TRBC1/2 targeting has considerable potential for immunotherapy of T-

329 cell malignancies. The principle of using immunotherapy to target a rearranged

330 clone-specific receptor is not new: Stevenson *et al* pioneered the use of patient-

331 specific anti-idiotype mAbs against neoplastic lymphoma cells[26,27]. However, this

332 approach is impracticable since it requires a novel binder to be generated for each

333 patient. An analogous approach to ours, targeting B-cell cancers with antibody light-

334 chain specific therapy has also been proposed[28].

335

336 Patients with B-cell malignancies have greatly benefited from the advent of potent

337 immunotherapies. Treatment of B-cell malignancies with anti-CD19 CART-cells has

338 been one of the most important recent advances in the treatment of cancer, with

339 sustained remissions obtained in most patients with advanced and refractory B-

340 ALL[6,29], as well as impressive though lesser responses in CLL[7,30] and diffuse large B-

341 cell lymphoma[7]. Given the relatively similar presentation and nature of B- and T-cell

342 malignancies, CART-cells could potentially have similar value in treating T-cell

343 lymphomas.

344

345 However, anti-CD19 CART efficacy is accompanied by loss of the normal B-cell

346 compartment[6,7]. While this is relatively well tolerated, and impact can be lessened by

347 infusion of donor–derived pooled immunoglobulins, analogously targeting a pan-T-

348 cell antigen on a T-cell malignancy (with concomitant permanent loss of normal T-

349 cells) would be prohibitively toxic, with no mitigating replacement therapies available.

350

351 Approaches using CARs against T-cell targets such as the pan T-cell antigen CD5[31]

352 or CD4, which is present on a crucial subset of normal T-cells[32], have been

353 proposed, but may prove unacceptably immunosuppressive in clinical use. With our

354 approach, a patient treated with anti-TRBC1 CART would retain approximately 2/3 of

355 normal T-cells, with polyclonal anti-viral immunity likely preserved. In addition, the

356 potential for 'on-target off-tumour' toxicity affecting other tissues would be negligible,

357 given the restriction of TCR expression to mature T- or NK/T-cells. However, with

358 any approach targeting T-cells rather than B-cells increased cytokine-mediated

359 toxicity could occur, due to lysis of normal tissue-resident T-cells and subsequent

360 mediator release. Another potential consequence of depletion of part of the

361 regulatory T-cell repertoire could be loss of some peripheral tolerance, if the T-

362 regulatory cells protecting a particular tissue were particularly skewed towards

363 TRBC1 or 2. However, ultimately the toxicities associated with depletion of TRBC1 or

364 2 cells could only be examined in a clinical trial.

365

366 In summary, we have demonstrated a novel approach to investigation and targeting

367 of T-cell malignancies by distinguishing between two possible TCR β-chain constant

368 regions. Using CART-cells targeting one constant region we have demonstrated

369 proof of concept. Exploration of the distribution of constant region usage by

370 unselected normal T-cells and those providing specific viral immunity suggests that

371 such an approach would not lead to significant immunosuppression. We hope that

372 this approach heralds the application of potent targeted immunotherapeutics to

373 provide much needed enhancement of the treatment of T-cell malignancies.

374

375

388

389

390

391

AUTHOR CONTRIBUTIONS

393 P.M.M. designed and performed the experimental work and wrote the manuscript.
394 P.A.W. performed experimental work. B.P. designed and performed *in vivo*
395 experiments. I.R. generated and tested EBV-CTLs. A.U.A. performed
396 immunohistochemistry. S.C.O., D.K.C. and AS produced soluble TCR molecules,
397 performed surface plasmon resonance analysis and wrote the manuscript. M.L. and
398 A.K.S. identified and characterised iNKTs. G.G., J.S. and M.A.Piris supplied clinical
399 samples. K.S.P. and D.C.L. provided advice and support and wrote the manuscript.
400 T.M. optimised and analysed immunohistochemical staining, and wrote the
401 manuscript. M.A.Pule conceived the idea, designed the experimental work and wrote
402 the manuscript.

403

404

COMPETING FINANCIAL INTEREST STATEMENT

406

407 P.M.M. and M.A.Pule have patent rights to targeting of TRBC for diagnosis and
408 treatment of T-cell malignancies (WO 2015132598 A1). P.M.M., BP, S.C.O., K.S.P.,
409 D.C.L. and M.A.Pule are shareholders in Autolus which has licensed anti-TRBC1
410 technology. S.C.O. and M.A.Pule are employees of Autolus which has licensed anti-
411 TRBC1 technology.

412

413

414   **REFERENCES**

415

416   1.   A clinical evaluation of the International Lymphoma Study Group classification
417   of non-Hodgkin's lymphoma. The Non-Hodgkin's Lymphoma Classification
418   Project. *Blood* **89,** 3909–3918 (1997).
419   2.   Vose, J., Armitage, J., Weisenburger, D.International T-Cell Lymphoma
420   Project. International peripheral T-cell and natural killer/T-cell lymphoma study:
421   pathology findings and clinical outcomes. *Journal of Clinical Oncology* **26,**
422   4124–4130 (2008).
423   3.   Weisenburger, D. D. *et al.* Peripheral T-cell lymphoma, not otherwise
424   specified: a report of 340 cases from the International Peripheral T-cell
425   Lymphoma Project. *Blood* **117,** 3402–3408 (2011).
426   4.   Gao, G. *et al.* A systematic review and meta-analysis of immunochemotherapy
427   with rituximab for B-cell non-Hodgkin's lymphoma. *Acta Oncol* **49,** 3–12
428   (2010).
429   5.   Bargou, R. *et al.* Tumor regression in cancer patients by very low doses of a T
430   cell-engaging antibody. *Science* **321,** 974–977 (2008).
431   6.   Maude, S. L. *et al.* Chimeric Antigen Receptor T Cells for Sustained
432   Remissions in Leukemia. *N Engl J Med* **371,** 1507–1517 (2014).
433   7.   Kochenderfer, J. N. *et al.* Chemotherapy-refractory diffuse large B-cell
434   lymphoma and indolent B-cell malignancies can be effectively treated with
435   autologous T cells expressing an anti-CD19 chimeric antigen receptor. *Journal
436   of Clinical Oncology* **33,** 540–549 (2015).
437   8.   Went, P. *et al.* Marker expression in peripheral T-cell lymphoma: a proposed
438   clinical-pathologic prognostic score. *Journal of Clinical Oncology* **24,** 2472–
439   2479 (2006).
440   9.   Notarangelo, L. D., Kim, M.-S., Walter, J. E. & Lee, Y. N. Human RAG
441   mutations: biochemistry and clinical implications. *Nat Rev Immunol* **16,** 234–
442   246 (2016).
443   10.   Pui, C. H. *et al.* Heterogeneity of presenting features and their relation to
444   treatment outcome in 120 children with T-cell acute lymphoblastic leukemia.
445   *Blood* **75,** 174–179 (1990).
446   11.   Jamal, S. *et al.* Immunophenotypic analysis of peripheral T-cell neoplasms. A
447   multiparameter flow cytometric approach. *Am. J. Clin. Pathol.* **116,** 512–526
448   (2001).
449   12.   Palomero, T. *et al.* Recurrent mutations in epigenetic regulators, RHOA and
450   FYN kinase in peripheral T cell lymphomas. *Sci Rep* **46,** 166–170 (2014).
451   13.   Delves, P. J., Martin, S. J. & Roitt, D. R. B. A. I. M. Roitt's Essential
452   Immunology. 1–562 (2011).
453   14.   Sims, J. E., Tunnacliffe, A., Smith, W. J. & Rabbitts, T. H. Complexity of
454   human T-cell antigen receptor beta-chain constant- and variable-region genes.
455   *Nature* **312,** 541–545 (1984).
456   15.   Tunnacliffe, A., Kefford, R., Milstein, C., Forster, A. & Rabbitts, T. H.
457   Sequence and evolution of the human T-cell antigen receptor beta-chain
458   genes. *Proc. Natl. Acad. Sci. U.S.A.* **82,** 5068–5072 (1985).
459   16.   Dickinson, A. M. *et al.* In situ dissection of the graft-versus-host activities of
460   cytotoxic T cells specific for minor histocompatibility antigens. *Nat. Med.* **8,**
461   410–414 (2002).
462   17.   Viney, J. L., Prosser, H. M., Hewitt, C. R., Lamb, J. R. & Owen, M. J.
463   Generation of monoclonal antibodies against a human T cell receptor beta
464   chain expressed in transgenic mice. *Hybridoma* **11,** 701–713 (1992).
465   18.   Reff, M. E. *et al.* Depletion of B cells in vivo by a chimeric mouse human
466   monoclonal antibody to CD20. *Blood* **83,** 435–445 (1994).
467   19.   Ricciardelli, I. *et al.* Towards gene therapy for EBV-associated posttransplant

468   lymphoma with genetically modified EBV-specific cytotoxic T cells. *Blood* **124,**
469   2514–2522 (2014).

470   20.   Swerdlow, S. H., International Agency for Research on CancerWorld Health
471   Organization. *WHO Classification of Tumours of Haematopoietic and*
472   *Lymphoid Tissues.* (International Agency for Research on Cancer, 2008).

473   21.   Pule, M. *et al.* A chimeric T cell antigen receptor that augments cytokine
474   release and supports clonal expansion of primary human T cells. *Molecular*
475   *Therapy* **12,** 933–941 (2005).

476   22.   Philip, B. *et al.* A highly compact epitope-based marker/suicide gene for easier
477   and safer T-cell therapy. *Blood* **124,** 1277–1287 (2014).

478   23.   Freeman, J. D., Warren, R. L., Webb, J. R., Nelson, B. H. & Holt, R. A.
479   Profiling the T-cell receptor beta-chain repertoire by massively parallel
480   sequencing. *Genome Research* **19,** 1817–1824 (2009).

481   24.   Rosenberg, W. M., Moss, P. A. & Bell, J. I. Variation in human T cell receptor
482   V beta and J beta repertoire: analysis using anchor polymerase chain reaction.
483   *Eur. J. Immunol.* **22,** 541–549 (1992).

484   25.   Brüggemann, M. *et al.* Powerful strategy for polymerase chain reaction-based
485   clonality assessment in T-cell malignancies Report of the BIOMED-2
486   Concerted Action BHM4 CT98-3936. *Leukemia* **21,** 215–221 (2006).

487   26.   Stevenson, F. K. *et al.* Antibodies to shared idiotypes as agents for analysis
488   and therapy for human B cell tumors. *Blood* **68,** 430–436 (1986).

489   27.   Hamblin, T. J. *et al.* Initial experience in treating human lymphoma with a
490   chimeric univalent derivative of monoclonal anti-idiotype antibody. *Blood* **69,**
491   790–797 (1987).

492   28.   Ramos, C. A. *et al.* Clinical responses with T lymphocytes targeting
493   malignancy-associated κ light chains. *J. Clin. Invest.* **126,** 1–9 (2016).

494   29.   Davila, M. L. *et al.* Efficacy and toxicity management of 19-28z CAR T cell
495   therapy in B cell acute lymphoblastic leukemia. *Sci Transl Med* **6,** 224ra25–
496   224ra25 (2014).

497   30.   Porter, D. L., Levine, B. L., Kalos, M., Bagg, A. & June, C. H. Chimeric antigen
498   receptor–modified T cells in chronic lymphoid leukemia. *N Engl J Med* **365,**
499   725–733 (2011).

500   31.   Mamonkin, M., Rouce, R. H., Tashiro, H. & Brenner, M. K. A T-cell-directed
501   chimeric antigen receptor for the selective treatment of T-cell malignancies.
502   *Blood* **126,** 983–992 (2015).

503   32.   Pinz, K. *et al.* Preclinical targeting of human T-cell malignancies using CD4-
504   specific chimeric antigen receptor (CAR)-engineered T cells. *Leukemia* **30,**
505   701–707 (2016).

506   33.   Boulter, J. M. *et al.* Stable, soluble T-cell receptor molecules for crystallization
507   and therapeutics. *Protein Eng.* **16,** 707–711 (2003).

508   34.   Garboczi, D. N. *et al.* Assembly, specific binding, and crystallization of a
509   human TCR-alphabeta with an antigenic Tax peptide from human T
510   lymphotropic virus type 1 and the class I MHC molecule HLA-A2. *J. Immunol.*
511   **157,** 5403–5410 (1996).

512   35.   Wyer, J. R. *et al.* T cell receptor and coreceptor CD8 alphaalpha bind peptide-
513   MHC independently and with distinct kinetics. *Immunity* **10,** 219–225 (1999).

514   36.   Straathof, K. C. An inducible caspase 9 safety switch for T-cell therapy. *Blood*
515   **105,** 4247–4254 (2005).

516

517

518

519 **ONLINE METHODS**

520

521 **Cell lines**

522

523 293T and K562 cell lines were cultured in IMDM (Lonza, Basel, Switzerland)

524 supplemented with 10% FBS (FBS, HyClone, GE, Buckinghamshire, UK) and 2 mM

525 GlutaMax (Invitrogen, CA, USA). Jurkat, Jurkat TCR-KO (and engineered variants),

526 HD-Mar2, HPB-ALL, H9, T-ALL1, MJ, CCRF-CEM and HH cells were cultured in

527 complete RPMI (RPMI1640, Lonza, Basel, Switzerland), supplemented with 10%

528 FBS and 2 mM GlutaMax). Cells were maintained in a humidified atmosphere

529 containing 5% CO_2 at 37°C. All cell lines were routinely tested for mycoplasma and

530 for surface expression of target antigens. All cell lines were obtained from American

531 Tissue Culture Collection (ATCC), Deutsche Sammlung von Mikroorganismen und

532 Zellkulturen (DSMZ) or Public Heath England collections. Jurkat TCR-KO cells were

533 a kind gift from the laboratory of Professor Hans Stauss.

534

535

536 **Cloning, expression and purification of TCR protein.**

537

538 The C5861 TCR expressing a TRBC2 domain[33] and the ILA1 TCR expressing a

539 TRBC1 domain[34], constructed using a disulphide-linked construct, were used to

540 produce the soluble α- and β- chain domains (variable and constant) for each TCR.

541 The TCRα and TCRβ chains were inserted into separate pGMT7 expression

542 plasmids under the control of the T7 promoter. Competent Rosetta DE3 *E. Coli* cells

543 (Merck, Darmstadt, Germany) were used to produce the C5861 and ILA1 TCRs in

544 the form of inclusion bodies using 0.5M IPTG to induce expression. Soluble C5861

545 and ILA1 TCRs were refolded as previously described[33] purified by anion exchange

546 (Poros 50HQ, Life Technologies, Cheshire, UK) and size exclusion chromatography

547 (S200 GR, GE Healthcare, Buckinghamshire, U.K.).

548

549 **Surface Plasmon Resonance (SPR) analysis**

550

551 The binding analysis was performed using a Biacore T200 (GE Healthcare,

552 Buckinghamshire, UK) equipped with a CM5 sensor chip as previously reported[35].

553 Briefly, 500-1000 Response Units (RUs) of JOVI-1 antibody was linked by amine

554 coupling to the chip surface. For the C5861 TRBC2 TCR, ten serial dilutions were

555 injected over the immobilised JOVI-1 and equibilibrium binding analysis was

556   performed. The equilibrium-binding constant (K_D (E)) values were calculated using a

557   nonlinear curve fit (y = (P1x)/(P2+x)). For the ILA1 TRBC1 TCR, single kinetic

558   injections were performed. For kinetics analysis, the K_{on} and K_{off} values were

559   calculated assuming 1:1 Langmuir binding and the data were analysed using a global

560   fit algorithm (BIAevaluation 3.1™).

561

562   **Cell staining and flow cytometry**

563

564   Flow cytometry was performed using BD LSR Fortessa instrument (BD, NJ, USA).

565   FACS sorting was performed using BD FACSAria (BD, NJ, USA). Staining steps

566   were performed at room temperature for 20 minutes, with PBS washes between

567   steps. For staining of intracellular antigens cells were fixed and permeabilised with

568   100uL of Cytofix/ Cytoperm (BD, NJ, USA) for 5 minutes prior to staining, and wash

569   steps were performed using PermWash (BD, NJ, USA). The following antibodies

570   were used (all anti-human unless otherwise specified, clone identity in brackets):

571   CD2 (TS1/8), CD3 (UCHT1), CD4 (OKT4), CD5 (UCHT2), CD7 (CD7-6B7), CD8

572   (SK1), human/ murine CD11b (M1/70), CD14 (M5E2), CD19 (HIB19), CD25 (BC96),

573   CD45 (HI30), CD45RA (HI100), CD56 (HCD56), CD57 (HCD57), CCR7 (GO43H7),

574   TCR α/β (T10B9), all from Biolegend, San Diego, CA, USA; CD34 (Qbend10, R&D

575   Systems, Oxford, UK); TRBC1 (JOVI-1, Ansell, Bayport, MN, USA), fixable viability

576   dye (eBioscience, ThermoFisher, Waltham, MA, USA). Anti-TRBC1 CAR expression

577   was detected by staining for RQR8 marker gene[22] with anti-CD34, or anti-MuFab

578   (115-116-072, Jackson Immuno, Westgrove, PA, USA). All antibodies other than

579   JOVI-1 were validated by manufacturer for diagnostic use. At least 5000 target

580   events were acquired per sample. Analyses were conducted using FlowJo v10

581   (Treestar, Ashland, OR, USA).

582

583

584   **Normal donors and viral peptide stimulation assays**

585

586   Approval for this study was obtained from the National Research Ethics Service,

587   Research Ethics Committee 4 (REC Reference number 09/H0715/64). All normal

588   donors provided informed consent.

589

590   PBMCs from unselected heathy donors were isolated by Ficoll-Paque (GE

591   Healthcare, Buckinghamshire, UK) gradient centrifugation, then were resuspended at

592   2×10^6 cells/ml in 1ml complete media in wells of a 24-well plate. Overlapping

593   peptide pools (15-mer, 11-mer overlap) derived from commonly immunogenic viral

594   proteins were obtained from JPT Technologies (Berlin, Germany, USA). The viruses

595   investigated (protein antigens in brackets) were cytomegalovirus, CMV (PP65) and

596   adenovirus, AdV (hexon and penton). Peptide pools were supplied as dried pellets

597   containing 25 μg/peptide and were reconstituted in 50μL DMSO. To obtain a final

598   concentration of 1μg/peptide/ml, 2μl of each peptide pool was added to each well of

599   PBMCs.

600

601   After 1hr initial incubation, brefeldin A (BD, NJ, USA) was added to prevent Golgi

602   transport. After a further 14hrs of culture, the cells were washed and surface staining

603   was performed for viability, CD4 and CD8. The cells were then washed and lysed/

604   permeabilised, then stained for intracellular interferon-γ, CD3 and JOVI-1 before

605   resuspension for FACS analysis. Negative control peptide pool (actin, a ubiquitous

606   cytoskeletal protein) and positive control (PMA/ ionomycin, Sigma Aldrich,

607   Darmstadt, Germany) conditions were included. Low-frequency viral-specific T-cells

608   were identified by intracellular interferon-gamma expression, with positive response

609   threshold set as >0.01% above negative control staining.

610

611   **Identification of T-cell diiferentiation subsets and mucosal-associated invariate**

612   **T-cells (MAITs) in normal donor peripheral blood**

613

614   Cells were defined as: naïve (CD45RA+CD45RO-CCR7-CD62L-), central memory

615   (CD45RA-CD45RO+CCR7+CD62L+), effector memory (CD45RA-CD45RO+CCR7-

616   CD62L-) and effector (CD45RA-CD45RO+CCR7+CD62L+) and T-regulatory cells

617   (CD4+FOXP3+CD25+). MAITs were identified as CD3+CD8+CD4-CD161+TCR-

618   Vα7.2 +ve.

619

620   **Invariant Natural Killer T-cell (iNKT) isolation**

621

622   Peripheral blood mononuclear cells (PBMC) were isolated from healthy donor blood

623   bags (Welsh Blood Service) using standard density gradient centrifugation. iNKT

624   cells were purified from PBMC by magnetic separation using anti-iNKT TCR beads

625   (Miltenyi Biotec) according to manufacturer's recommendations. The purified cell

626   fraction was subsequently expanded with phytohaemagglutinin and allogeneic

627   irradiated feeders from three donors. After a minimum of 14 days post expansion,

628   cells were phenotyped and used in functional assays.

629

630 Molt-3 cell line (endogenously expressing CD1d) was pulsed overnight with 100

631 ng/ml α-galactosylceramide (αGalCer, Sigma). iNKT lines were subsequently co-

632 incubated with Molt-3 pulsed with αGalCer for 5 hours in presence of monensin,

633 brefeldin A and CD107a antibody (all from BD Biosciences), according to

634 manufacturer's recommendations. iNKT lines were also incubated with media only,

635 and with Molt-3 pulsed with vehicle only (DMSO). iNKTs were identified by

636 upregulation of CD107a and IFN-γ in response to Molt-3 pulsed with αGalCer.

637

638

639 **Retroviral transduction of T-cells**

640

641 RD114-pseudotyped supernatant was generated as follows: 293T cells were

642 transfected with vector plasmid; RDF, an expression plasmid to supply RD114

643 envelope (gift of Mary Collins, University College London); and PeqPam-env, a

644 gagpol expression plasmid (gift of Elio Vanin, Baylor College of Medicine).

645 Transfection was facilitated using Genejuice (Merck, Darmstad, Germany).

646 Peripheral blood mononuclear cell transductions were performed as follows: T cells

647 from normal donors were isolated by Ficoll (GE, Buckinghamshire, UK) gradient

648 centrifugation and stimulated with phytohemagglutinin (Sigma Aldrich, Darmstadt,

649 Germany) at 5mg/mL. Interleukin-2 (IL-2, Genscript, Nanjing, China) stimulation (100

650 IU/mL) was added following overnight stimulation. On day 3, T cells were harvested,

651 plated on retronectin (Takara, Nojihigashi, Japan) and retroviral supernatant, and

652 centrifuged at 1000g for 40 minutes. Transduction efficiency was determined on D6-7

653 following initial harvest and further experiments were commenced on D7-10 following

654 initial harvest. PBMCs were maintained in complete RPMI.

655

656 **Generation and cytotoxicity assessment of EBV-specific CTLs**

657

658 This was performed as previously described[19]. Briefly, PBMCs from a normal donor

659 were infected with EBV resulting in B-cell transformation to produce immortalised

660 lymphoblastoid cells. These cells were irradiated and used as target cells to stimulate

661 untransfomed PBMCs from the same donor, selectively expanding EBV-specific

662 CTLs over a 23-day period. Cytotoxicity of EBV-CTLs against K562 cell line (an

663 erythroleukaemia cell line with loss of MHC class 1 expression), allogeneic and

664 autologous lymphoblastoid cells was assessed using standard 4hr chromium release

665 cytotoxicity assays as previously described[36].

666

667

668 **Preparation and staining of primary tumour samples for FACS or**
669 **immunohistochemistry**

670

671 Approval for this study was obtained from the National Research Ethics Service,
672 Research Ethics Committee 4 (REC Reference number 09/H0715/64). Informed
673 consent was obtained from all patients. For FACS, PBMCs from patients with T-cell
674 malignancies were obtained from whole blood or marrow samples by Ficoll-Paque
675 (GE Healthcare, Buckinghamshire, UK) gradient centrifugation prior to staining and
676 analysis as above. Gating strategies to identify malignant and healthy T-cells were
677 determined on a patient-specific basis according to data previously obtained by
678 primary clinical laboratories. For immunohistochemistry, fresh biopsy samples of
679 patients with a range of T-cell malignancies (see Figure 3f) were snap-frozen in liquid
680 nitrogen and tissue sections were prepared according to standard methodology. The
681 investigated antibodies included the mouse monoclonal anti-T Cell Receptor Beta 1
682 (clone JOVI.1; Ancell Corporation, Bayport, MN, USA) and the mouse monoclonal
683 anti-TCR beta F1 (clone 8A3; Thermo Fisher Scientific, Loughborough, UK). The
684 antibodies were assessed under different conditions (i.e. dilution and antigen
685 retrieval protocol) and the chosen dilution which showed selective background-free
686 reaction in fresh tissue sections of human reactive tonsils (nr. 2) used as positive
687 control were 1:5000 for JOVI.1 and 1:50 for TCR Beta F1 respectively. The staining
688 procedure was performed using the Roche-Ventana BenchMark Ultra autostainer
689 (Ventana Medical System, Tuscon, US). Counterstaining was performed using
690 haematoxylin and bluing reagent from Ventana/Roche; slides were mounted with
691 cover slips and air-dried.

692

693

694 **Chromium release cytotoxicity assays**

695

696 Standard 4hr chromium release cytotoxicity assays were performed as previously
697 described[36], with all assays performed in triplicate. NK cell depletion was performed
698 prior to assays using CD56 magnetic bead depletion and LD columns (Miltenyi,
699 Begisch Gladbach, Germany).

700

701 **FACS-based co-culture and cytotoxicity assays**

702

703   Target and effector cells were resuspended at 1M cells/ml in complete media. 50-

704   100uL of each cell suspension was added to wells of a V-bottom 96-well plate to

705   achieve a 1:1 E:T ratio with 50 000 or 100 000 targets/ well. For some experiments

706   target cell were pre-labelled with carboxyfluorescein succinimidyl ester (CFSE) or

707   CellTrace Violet (CTV, both Invitrogen, Carlsbad, CA, USA) dyes according to

708   manufacturer's instructions. The plate was placed in a standard cell culture incubator

709   containing 5% CO_2 at 37°C. After 24hrs the plate was spun down at 400G for 5mins,

710   100uL of supernatant was removed for cytokine assays and replaced with fresh

711   complete media. At 48hrs or 7 days, the plate was spun down at 400G for 5mins and

712   supernatant was decanted. 100uL of staining cocktail (appropriate antibodies/

713   viability dye (eBioscience, ThermoFisher, Waltham, MA, USA) diluted in PBS) was

714   added and cells were stained for 20mins in the dark at room temperature. Wells

715   were then washed with a further 100uL of PBS and spun down at 400G for 5 mins.

716   Supernatant was decanted. Counting beads (Flow check fluorospheres, BD, NJ,

717   USA) were washed in PBS then resuspended at 1M beads/ ml in PBS. 100uL of

718   PBS/ counting bead mixture was added to each cells (10 000 beads/ well). 2000

719   beads were acquired per sample. Gating on single live target cells was performed

720   according to exclusion of fixable viability dye, forward and side scatter characteristics

721   and expression of fluorescent protein, marker gene or fluorescent dye. Assays were

722   performed in triplicate. % cytotoxicity was calculated as: 10000/ number of beads

723   collected x number of target cells at end/ number of target cells at start of culture x

724   100.

725

726   For primary cancer cell killing experiments, allogeneic T-cells were typically used as

727   effectors, other than in Figure 4j-l where cryopreserved normal patient T-cells were

728   used. Bespoke gating strategies were used to identify normal and malignant T-cells

729   in each patient sample.

730

731   **Cell sorting with magnetic bead selection**

732

733   Transduced T-cells positive or negative for the RQR8 marker gene (contains

734   Qbend10-CD34 epitope) were selected by positive or negative bead selection

735   according to the manufacturer' instructions (Miltenyi, Bergisch Gladbach, Germany)

736   using MS or LD columns respectively. For TRBC1 T-cell positive or negative

737   selection, cells were initially stained with JOVI-1-biotin then incubated with

738   streptavidin-conjugated magnetic beads, then separated according to the

739   manufacturer's instructions. To increase purity a second selection/ depletion round

740   was performed.

741

Murine models of T-cell malignancy

743

744   This work was performed under United Kingdom home-office–approved project

745   license and was approved by University College London Biological Services Ethical

746   Review Committee. 6-8-week-old male non-obese diabetic-severe combined

747   immunodeficiency γ-chain–deficient (NSG) mice (Jackson Laboratory, Bar Harbor,

748   ME, USA) were intravenously injected via the tail vein with Jurkat cells, human

749   PBMCs or CAR T-cells as described in the text. An otherwise identical irrelevant

750   control CAR targeting B-cell maturation antigen (BCMA), which is not expressed in T-

751   cell malignancies, was used in some experiments as indicated in the text. Tail vein

752   bleeds of 50uL were undertaken as indicated in the text. At the time of cull, in some

753   experiments bone marrow was harvested. Single cell suspensions were prepared

754   and analysed for presence of T-cells and residual Jurkat cells by flow cytometry.

755   Jurkat cells were identified by CD19 or BFP marker gene according to experiment.

756   CAR T-cells were identified by expression of RQR8 marker gene.

757

758   For experiments with a survival endpoint or engraftment of PBMCs, mice were

759   monitored with at least twice weekly weighing. Animals with >10% weight loss or

760   those displaying evidence of GvHD or disease progression including hunched

761   posture, poor coat condition, reduced mobility, pilorection or hind limb paralysis were

762   culled.

763

764   Bioluminescent imaging of mice was performed using IVIS system (Perkin Elmer,

765   Buckinghamshire, UK). Prior to imaging, animals were placed in an anesthetic

766   chamber. General anesthesia was induced using inhaled isoflurane. Following

767   induction, intraperitoneal injection of luciferin (200uL via 27G needle) was

768   undertaken. After 2 minutes, mice were placed in the imaging chamber.

769   Simultaneous optical and bioluminescent imaging was performed. Anaesthesia was

770   maintained by continued inhalation of isoflurane during imaging.

771

Statistical analyses

773

774   Unless otherwise noted, data are summarised as mean $\pm$ SEM. Student's *t*-test was

775   used to determine statistically significant differences between samples for normally

776   distributed variables, with Mann-Whitney U-test used for non-parametrically

777   distributed variables. p < 0.05 (2-tailed) indicated a significant difference. Unless

778   otherwise stated, variances were similar between study populations. When variances

779   were unequal, Welch's correction for unequal variance was used. Paired analyses

780   were used when appropriate. When 3 groups were compared, 1-way ANOVA with

781   Dunnett's test for multiple comparisons with alpha of 0.05 were used. When multiple

782   t-tests were performed, statistical significance was determined using the Holm-Sidak

783   method with alpha of 0.05. Neither randomisation nor blinding was done during the *in*

784   *vivo* study. However, mice were matched based on the luminescent signal for control

785   and treatment groups before infusion of control or gene-modified T-cells. Cohort

786   sizes were based on number required to demonstrate 90% reduction in

787   bioluminescence, 95% confidence with 80% power. Survival curves were generated

788   using the Kaplan-Meier method with hazard ratios calculated by Mantel-Haenszel

789   method. All animal studies were performed at least twice, with data presented

790   representing one representative experiment. Graph generation and statistical

791   analyses were performed using Prism version 7.0b software (GraphPad, La Jolla, CA

792

793   Further details can be found in Life Sciences Reporting Summary accompanying the

794   online version of this manuscript.

795

796

797   FIGURE LEGENDS

798

799

800   **Figure 1:** Differential detection of TRBC1 but not TRBC2 by JOVI-1 antibody. (a)

801   Proposed structure of the TCR-CD3 complex assembled on T-cell surface (β-

802   constant region highlighted in dotted box) (b) The process of β-gene re-arrangement

803   involving specific VDJ(C) recombination (c) Alignment of TRBC1 and TRBC2 protein

804   sequences, differences highlighted in red (d) Staining of NT and engineered TRBC1-

805   JKO, TRBC2-JKO cell lines with CD3 and JOVI-1 antibodies (e) JOVI-1 staining of

806   HEK-293T cells, transfected to express TCRs with varying specificities and TRB-VDJ

807   usage (gated on CD3+ cells) (f) JOVI-1 staining of engineered JKO cell lines

808   transduced to stably express truncated TCRs lacking V(D)J regions, or each

809   difference between TRBC1 and TRBC2 introduced individually. Gated on CD3+ cells.

810   (g) 3D representation of discriminating TRBC1 and TRBC2 epitopes on the surface

811   of TRBC. Asparagine (Asn, N) and lysine (Lys, K) residues are highlighted, with

812 exposed lysine residue in TRBC1 epitope indicated by black arrow. TCR = T-cell

813 receptor; VDJC = variable, diversity, joining, constant; JKO = Jurkat T-cell receptor

814 knockout., NT = non-transduced

815

816

817 **Figure 2:** Unselected polyclonal and viral-specific T-cells contain both TRBC1-

818 positive and TRBC1-negative populations. (a) Staining of representative normal

819 donor CD4 (left) and CD8 (right) T-cells with TCR and JOVI-1 antibodies (b)

820 Proportion of normal T-cells expressing TRBC1 in CD4 and CD8 compartments,

821 summary data from 27 normal donors. Lines = mean, standard deviation. (c)

822 TRBC1+:TRBC1- proportion of EBV-CTLs in 3 normal donors (d) Staining of viral-

823 specific T-cells with CD3 and JOVI-1, data from one representative normal donor

824 shown (e) TRBC1 expression in viral-specific cells, summary data from 3 (CMV) and

825 5 (AdV) normal donors. Lines = median. TCR = T-cell receptor, EBV = Epstein Barr

826 virus, CTL = cytotoxic T-lymphocyte, CMV = cytomegalovirus, AdV = adenovirus,

827 IFN-G = interferon gamma.

828

829

830 **Figure 3:** T-cell derived cell lines and primary T-cell malignancies are monoclonally

831 TRBC1-positive or TRBC1-negative. (a) Staining of TCR-positive cell lines with JOVI-

832 1 (left), with matched sequencing traces of TCR-β constant region (right). (b) Flow

833 cytometry of normal and malignant T-cells from 2 representative patients with T-LGL

834 (total 4 T-LGL samples examined, 1 TRBC1+, 3 TRBC1-). Top = TRBC1-positive,

835 bottom = TRBC1-negative. T-LGL gating = TCR+CD4-CD8+CD57+. TRBC1-

836 negative cells in top panel T-LGL gate likely reflect normal CD8+CD57+ T-cells,

837 monoclonality suggested by elevated TRBC1+:TRBC1- ratio. (c) Flow cytometry of

838 normal and malignant T-cells from 2 representative patients with T-ALL. Top =

839 TRBC1-positive, bottom = TRBC1-negative. Blasts = CD3(intra)+CD4+CD8+. (d)

840 Staining of frozen sections of TCR-positive TRBC1-negative lymphoma with TCR

841 (left) and JOVI-1 (right). TRBC1-positive T-cells likely to represent contaminating

842 healthy T-cells. Histology: A = T-acute lymphoblastic leukaemia (T-ALL), B =

843 angioimmunoblastic T-cell lymphoma (AITL), C = AITL (e) Staining of frozen sections

844 of TCR-positive TRBC1-positive lymphoma with TCR (left) and JOVI-1 (right). A =

845 anaplastic large cell lymphoma (ALCL), B = T-ALL, C = peripheral T-cell lymphoma

846 not otherwise specified (PTCL-NOS). Positive cells in d,e stain brown, scale bars =

847 250μM. (f) TCR expression on malignant cells and TRBC1-positive cell lines.

848   Malignant cell expression of TCR quantified by MFI on FACS, expressed as % TCR

849   expression on normal T-cells from the same patient. Grey triangles = cases of ATLL,

850   other histologies = black circles. Red triangle = Jurkat cell line. T-LGL = T-large

851   granular lymphocytosis, MFI = median fluorescence intensity.

852

853

854

855   **Figure 4:** Anti-TRBC1 CART-cells are effective and specific against TRBC1+ cell

856   lines and primary T-cell malignancies *in vitro.* (a) Example anti-TRBC1 CAR

857   transduction, repeated in >10 donors, assessed by anti-Fab staining for CAR. (b)

858   Interferon-γ secretion by NT or anti-TRBC1 CAR T-cells against TRBC1-JKO cells,

859   24-hour co-culture, donor n=6, *p<0.0001 for paired t-test v NT effectors. (c)

860   Interferon-γ secretion by anti-TRBC1 CAR T-cells against NT-JKO, TRBC1-JKO or

861   TRBC2-JKO cells, 24-hour co-culture, donor n=6, *p<0.0001, 1-way ANOVA and

862   Dunnett's test for multiple comparisons v NT-JKO target cells. (d) Killing of TRBC1-

863   JKO cells by NT or anti-TRBC1 CART-cells, 4hr chromium-release assay, 16:1 E:T

864   ratio, donor n=3, *p<0.001, paired t-test v NT effectors. (e) Killing of TRBC1-JKO or

865   TRBC2-JKO cells by anti-TRBC1 CART-cells, 4hr chromium-release assay, 16:1 E:T

866   ratio, donor n=3, *p<0.05, 1-way ANOVA and Dunnett's test for multiple comparisons

867   v NT-JKO target cells. (f) Flow-based cytotoxicity assay, target cells expressed as %

868   of starting cells after 48hrs, donor n=2, 3 replicates per donor, *corrected p<0.01 for

869   comparison v NT effectors, unpaired t-tests with Holm-Sidak correction for multiple

870   comparisons. (g) Co-culture of mixed TRBC1/ TRBC2 cells, representative FACS

871   plot at 48hrs. Numbers on plots = absolute numbers of events. (h) Primary TRBC1+

872   malignant samples with residual normal CD8 T-cells after 120hr co-culture with NT or

873   anti-TRBC1 allogeneic CAR T-cells. Left = T-PLL, malignant cells = CD7bright CD4+.

874   Right panel = PTCL-NOS. Malignant cells = CD4brightCD7-. (i) Primary ATLL

875   sample after 120hr co-culture with allogeneic NT or anti-TRBC1 CAR T-cells.

876   Malignant cells = CD3dimCD8+CD7-. (j) Transduction of PBMCs from patient with

877   ATLL, assessed by RQR8 marker gene. (k) Malignant cell burden following

878   transduction with anti-TRBC1 CAR. (l) Primary ATLL sample after 120hr co-culture

879   with autologous NT or anti-TRBC1 CAR T-cells. Malignant cell gating =

880   CD2+CD4+CD7-CD8-. All experiments other than in j-l used effector T-cells from

881   normal donors. Lines on graphs b,d = mean. Whiskers on graphs c,e = range, box =

882   25th-75th centile. Numbers on flow plots represent % of events in a,h,i,j,k,l. NT = non-

883   transduced, JKO = Jurkat T-cell receptor-knockout, CAR = chimeric antigen receptor,

884 BFP = blue fluorescent protein, ATLL = adult T-cell leukaemia/ lymphoma, T-PLL =

885 T-prolymphocytic leukaemia, PTCL-NOS = peripheral T-cell lymphoma, not

886 otherwise specified.

887

888

889 **Figure 5:** Efficacy and specificity of anti-TRBC1 CAR in Jurkat xenograft murine

890 models of T-cell malignancy. (a) Flow diagram of survival experiment (b)

891 Bioluminescence imaging at D-1 and D10 following CAR T-cell injection (c) Radiance

892 of individual animals at D10 following control or anti-TRBC1 CAR T-cell injection,

893 $p<0.0001$, Student's t-test (d) Kaplan-Meier survival curves of animals in survival

894 experiment (median OS 54 v 21 days, HR=0.037, $p<0.00001$, n=10/ group, log-rank

895 test) (e) Flow diagram of persistence experiment (f) Jurkat cell, total T-cell and CD8

896 CAR-T cell numbers from bleed at D21 following control CAR or anti-TRBC1 CAR T-

897 cell injection. CAR was detected by expression of RQR8 marker gene. (g) Numbers

898 of total T-cells and CD8 CAR T-cells in the bone marrow at time of cull (D42 in anti-

899 TRBC1 CAR recipients). Comparisons in f,g were made using Mann-Whitney U-test.

900 (h) Flow diagram of specificity experiment (i) Flow cytometry of bone marrow in mice

901 engrafted with equal proportions of TRBC1-Jurkat and TRBC2-JKO cells, following

902 treatment with NT or anti-TRBC1 CAR T-cells, representative examples. TRBC1

903 cells were detected by CD19 marker gene, TRBC2 cells were detected by BFP

904 marker gene (j) Quantification of TRBC1 proportion of residual target cells by flow

905 cytometry, n=5 per group, $*p=0.0003$ for TRBC1% of residual tumour, unpaired t-test

906 with Welch's correction for unequal variance v NT effectors. All experiments used

907 effector T-cells from healthy donors. Horizontal lines represent medians. $*p<0.05$,

908 $***p<0.001$. JKO = Jurkat T-cell receptor knockout, NT = non-transduced, CAR =

909 chimeric antigen receptor BFP = blue fluorescent protein.

910

911

912

913

914

915

916

917

918

919

920

Diagnosis	TRBC1+ (%)	TRBC1-	Total
Anaplastic large cell lymphoma	5 (42)	7	12
Angioimmunoblastic T-cell lymphoma	2 (40)	3	5
Peripheral T-cell lymphoma, NOS	8 (44)	10	18
NK/T-cell lymphoma	0 (0)	1	1
Sézary syndrome	1 (33)	2	3
T-acute lymphoblastic leukaemia/ lymphoma*	2 (25)	7	9
Adult T-cell leukaemia/ lymphoma*	2 (100)	0	2
T-prolymphocytic leukaemia*	1 (33)	2	3
T-large granular leukaemia*	1 (25)	3	4
OVERALL	**22 (39)**	**35**	**57**

921   **Table 1.** Summary data of TRBC1 expression in primary samples of T-cell receptor-
922   positive malignancies. *cases mainly assessed by flow cytometry, non-starred =
923   mainly assessed by immunohistochemistry. NOS = not otherwise specified

a

b
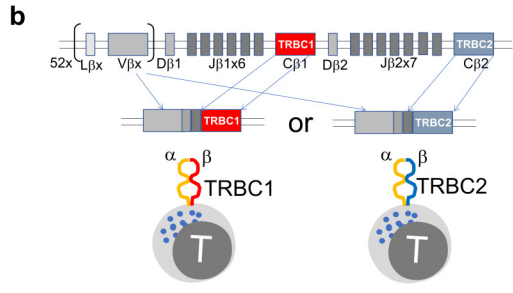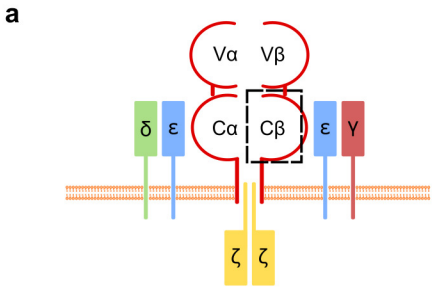
c

```
                NK-KN 4/5                            F-Y 36
TRBC1    1  EDLNKVFPPEVAVFEPSEAEISHTQKATLVCLATGFFPDHVELSWWVNGK
TRBC2    1  EDLKNVFPPEVAVFEPSEAEISHTQKATLVCLATGFYPDHVELSWWVNGK

TRBC1   51  EVHSGVSTDPQPLKEQPALNDSRYCLSSRLRVSATFWQNPRNHFRCQVQF
TRBC2   51  EVHSGVSTDPQPLKEQPALNDSRYCLSSRLRVSATFWQNPRNHFRCQVQF

TRBC1  101  YGLSENDEWTQDRAKPVTQIVSAEAWGRADCGFTSVSYQQGVLSAT
TRBC2  101  YGLSENDEWTQDRAKPVTQIVSAEAWGRADCGFTSESYQQGVLSAT
                                                  V-E 135
```

d

e

V7-3 D1-1 J2-3
V27-1 D2-1 J2-3
V6-2 D1-1 J2-4
V9-1 D1 J2-1
V20-1 D? J2-3
V6-5 D2 J2-7
V6-1 D2 J2-2
V6-5 D1 J1-2
V10-3 D1 J1-5
V6-6 D1-1 J1-3
V19-1 D1 J1-4
V28-1 D1 J1-2

JOVI-1

f

△TRBC2
△TRBC1
E-V, 135
Y-F, 36
KN-NK, 4-5
TRBC2
TRBC1
NT

JOVI-1

g

Asn-Lys (C1 epitope)   Lys-Asn (C2 epitope)

a

CD4

JOVI-1

TRBC1+
40.9
TRBC1−
58.1

CD8

TRBC1+
36.5
TRBC1−
62.7

TCR

b

% TRBC1 Cells

CD4   CD8

c

% of Total TCR+CD8+ Cells

TRBC1−
TRBC1+

1   2   3
Donor

d

CMV

JOVI-1

TRBC1+
53.3
TRBC1−
43.5

AdV

TRBC1+
53.6
TRBC1−
46.4

CD3

e

% TRBC1 Cells

CMV   AdV

a

TRBC1
TRBC2
MJ
Jurkat
H9
HPB-ALL
HH
T-ALL1
HD-Mar2
CCRF-CEM
JKO

JOVI-1

ACGGA
ACAGA

b

	CD4	CD8	T-LGL
	TRBC1+ 37.7	TRBC1+ 35.2	TRBC1+ 82.5
	TRBC1– 61.5	TRBC1– 62.5	TRBC1– 16.4
	TRBC1 44.7	TRBC1 32.1	TRBC1 1.99
	TRBC2 54.4	TRBC2 67.5	TRBC2 97.9

JOVI-1

TCR

c

	CD4	CD8	Blasts
	TRBC1+ 50.8	TRBC1+ 49.4	TRBC1+ 97.9
	TRBC1– 47.7	TRBC1– 48.7	TRBC1– 1.78
	TRBC1– 55.6	TRBC1– 45.9	TRBC1+ 0.72
	TRBC1– 43.0	TRBC1– 52.2	TRBC1– 95.8

JOVI-1

CD3

d

A TCRβ   JOVI-1
B TCRβ   JOVI-1
C TCRβ   JOVI-1

e

A TCRβ   JOVI-1
B TCRβ   JOVI-1
C TCRβ   JOVI-1

f

Tumour MFI (% of Normal T-Cell)

a

NT
CAR
CAR+
74.9
aFab

b

NT CAR
*
Interferon Gamma (pg/mL)

c

JKO TRBC1 TRBC2
*
Interferon Gamma (pg/mL)

d

NT CAR
*
% Maximal Killing

e

JKO TRBC1 TRBC2
*
% Maximal Killing

f

NT
CAR

Jurkat H9 MJ CCRF HH T-ALL1 HD-Mar2
*   *   *
−TRBC1− ──TRBC2──
% of starting cells

g

T-PLL

NT   CAR
CD8 42   CD8 43
T-PLL 5354   T-PLL 20
CD8   CD8
CD4

PTCL-NOS

NT   CAR
CD8 199   PTCL 6685   CD8 174   PTCL 14
CD4 401   CD4 83

h

ATLL

NT   CAR
ATLL 14.1   ATLL 0.56
CD8
CD3

i

NT   CAR
TRBC2 55.4   TRBC2 98.3
TRBC1 44.4   TRBC1 1.20
TRBC2 (BFP)
TRBC1 (CD19)

j

NT
CAR
CAR+
67.5
CAR

k

NT   CAR
ATLL 22.2   ATLL 3.7
CD7
CD4

l

Unstimulated   CAR
ATLL 47.7   ATLL 0.64
CD7
CD4

a

NSG

D-6	D0	2x/wk	D60
IV 3x10⁶ Jurkat -Fluc-CD19	IV 8x10⁵ CAR T		Cull survivors

b

Control CAR   Anti-TRBC CAR

D-1

D10

c

Radiance (Ph/s/cm²/sr)

***

Control   TRBC1

d

Fraction survival

Control

TRBC1

***

Time from CAR Injection (Days)

e

NSG

D-6	D0	2x/wk	D21	D42
IV 3x10⁶ Jurkat -Fluc-CD19	IV 8x10⁵ CAR T			Cull survivors

f

Blood

Jurkat (n/uL)   *
Control   TRBC1

T-Cells (n/uL)   *
Control   TRBC1

CD8+ CART-Cells (n/uL)   *
Control   TRBC1

g

Marrow

T-Cells (n)   *
Control   TRBC1

CD8+ CAR T-Cells (n)   *
Control   TRBC1

h

NSG

D-6	D0	D+6
IV 1.5 x10⁶ each Jurkat-CD19 JKO-TRBC2-BFP	IV 4 x10⁶ NT/ CAR T-cells	Cull

i

BFP (TRBC2)

NT   CAR

TRBC2 44.9   TRBC2 99.6

TRBC1 54.5   TRBC1 0.098

CD19 (TRBC1)

j

TRBC1+ % of Residual Jurkat

***

NT   CAR